Available online at www.sciencedirect.com
SCIENCE DIRECT®
Biochimica et Biophysica Acta 1660 (2004) 164–170
BIOCHIMICA ET BIOPHYSICA ACTA
BBA
www.bba-direct.com

The voltage-dependent nonselective cation current in human red blood cells studied by means of whole-cell and nystatin-perforated patch-clamp techniques

S. Rodighiero[1], A. De Simoni[2], A. Formenti*

Institute of Human Physiology II, University of Milano, Via Mangiagalli, 32, I-20133 Milano, Italy

Received 31 July 2003; received in revised form 10 November 2003; accepted 17 November 2003

Abstract

Human red blood cells (RBC) can be studied by means of whole-cell and nystatin-perforated patch-clamp techniques. In 85% of the whole-cell experiments ($n=86$) and 69% of the perforated-patch recordings ($n=13$), steps to positive potentials, from a holding potential of 0 mV, induced a slow-activating non-inactivating persistent outward current which reverted at about 0 mV. The current activation phase fitted well with a two-component exponential curve. Half-maximal conductance was reached at about 42 mV. Na^+ and K^+ carried this current, which was not affected by 20 nM charybdotoxin or 20 mM TEA, but was reduced following a partial substitution of extracellular Cl^- by tartrate. This current has characteristics similar to the single-channel currents already described in RBC and may be involved in the rapid adaptations of these cells in the circulation.

Keywords: Human red cell; Erythrocyte; Voltage-dependent nonselective cationic channel; Patch-clamp

1. Introduction

The permeability to cations of the human red blood cell (RBC) membrane increases when changes in the extracellular medium induce a more positive membrane potential. Although this effect has been known from quite a long time [1–3], it was not possible to explain why a membrane potential more positive than +40 mV could induce a pronounced increase in K^+ efflux. Based on tracer experiments, the presence of voltage-activated cation transport in human erythrocytes has been suggested [4]. This increased permeability is nonselective for Na^+ and K^+ and activates at membrane potentials positive to +40 mV. With the patch-clamp technique, using an inside-out configuration, it was possible to observe the presence of voltage-dependent nonselective cation channels (NSC) in the human RBC membrane [5]. However, the single-channel recordings were done at a very high KCl concentration (500 mM), and the authors noted that the open probability at physiological salt concentration was very low. Discrepancies in the data from the literature [5,6] regarding the membrane potential at which the channels begin to open were reconciled in a further paper [7] with the finding of a hysteresis-like open probability curve.

There are very few studies on human RBC using the whole-cell patch-clamp and perforated-patch technique. This is mainly because of the technical difficulties inherent to patch-clamping these cells. These methods allow recordings utilizing salt solutions at physiological concentrations. Furthermore, the channels formed by the nystatin in the perforated-patch, which are permeable to monovalent ions but exclude multivalent ions and molecules as large as or larger than glucose, avoid the dialysis of important substances from the erythrocyte's cytoplasm [8].

We report here that it is possible to obtain whole-cell and perforated-patch recordings of NSC currents in human

* Corresponding author. Tel.: +39-2-503-15464; fax: +39-2-700411620.
E-mail address: Alessandro.Formenti@unimi.it (A. Formenti).
[1] Present address: Dipartimento di Scienze Biomolecolari e Biotecnologie, Università di Milano, Italy.
[2] Present address: Department of Physiology, University College London, UK.

0005-2736/$ - see front matter © 2003 Elsevier B.V. All rights reserved.
doi:10.1016/j.bbamem.2003.11.011

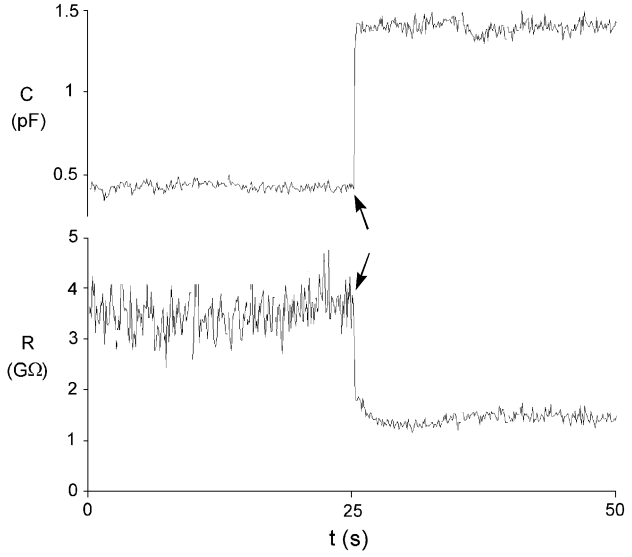

Fig. 1. A typical recording of the membrane capacitance (Cm) and resistance (Rm) during the transition (arrows) from cell-attached to whole-cell configuration in a human RBC. The sudden capacity increase during the whole-cell establishment is about 1 pF. The value observed is acceptable if we consider that a RBC has a cellular surface of about 160 μm^2 and we assume a standard capacity of 0.8–1.0 $\mu F/cm^2$, taking into account that part of the cell membrane is sealed to the microelectrode.

RBC, and using these techniques we analyse NSC characteristics at the whole cell level.

2. Materials and methods

2.1. Preparation of RBC

Blood was drawn from 11 healthy donors and collected in heparinized tubes. It was centrifuged in a refrigerated centrifuge (ALC, Italy) at 4 °C, 400 × *g* for 5 min, and washed three times with a washing solution containing (mM): 150 NaCl, 2 $MgCl_2$, 4 KCl, 10 HEPES, 10 glucose, pH 7.4.

RBC were diluted 1:400 in the bath solution used for the patch-clamp experiments and plated on uncoated Petri dishes. Contrary to poly-D-lysine coating that causes the RBC to adhere very tightly, these conditions allowed the cells to adhere loosely to the surface of the plate, keeping their physiological morphology.

2.2. Patch-clamp recordings

Recordings started a few minutes after plating, using the whole-cell patch-clamp technique [9]. Patch electrodes were fabricated from borosilicate capillary tubes (GC100-10, 1.0-mm outside diameter, 0.58-mm inside diameter; Clark Electromedical Instruments), with a resistance of about 15 MΩ when measured in a standard bath solution. Because of the red cell membrane's special resistance to mechanical stress [10], the most difficult step in obtaining the whole-cell configuration was the disruption of the patch area after GΩ seal formation. In about 30% of the attempts, the cell was completely sucked into the pipette. The achievement of a whole-cell configuration was accompanied by the sudden appearance of the membrane-capacitance current transients, prior to rupture compensated in cell-attached configuration. During the next few seconds, the cell became nearly transparent, presumably because of a gradual diffusion of the haemoglobin into the pipette. The membrane capacitance (Cm) and resistance (Rm) during the rupture of the membrane patch were evaluated by means of the Membrane-Test program (Axon Instruments, USA). The capacitive increment was 0.99 ± 0.29 pF ($n = 27$). Considering that standard Cm value is 0.8–1.0 $\mu F\ cm^{-2}$ for biological membranes, and the red cell membrane is about 163 μm^2, then Cm in a red cell should be about 1.30–1.63 pF. The smaller value observed can be explained taking into account that part of the cell is sucked into the pipette and its membrane is partially sealed to the pipette glass. Cm was not com-

Table 1
Solutions used for whole-cell and perforated-patch clamp recordings

	Ext. 1	Ext. 2	Ext. 3	Ext. 4	Ext. 5	Ext. 6	Int. 1	Int. 2	Int. 3	Int. 4
NaCl	150	150	38	4	4	130				4
Na_2tartrate			56							
KCl	4	4	4	4	150	4	140	140	55	4
$MgCl_2$	2	4	2	2	2	2	2	2	1	2
$CaCl_2$	2		2	2	2	2	1			1
K_2SO_4									25	
NMDG-Cl				146						132
TEACl						20				
EGTA							11	10		11
HEPES	10	10	10	10	10	10	10	10		10
NaHEPES									10	
Glucose	10	10	10	10	10	10				
Sucrose			56							
PH	7.4 (NaOH)	7.4 (NaOH)	7.4 (NaOH)	7.4 (NMDG)	7.4 (KOH)	7.4 (NaOH)	7.2 (KOH)	7.2 (KOH)	7.2 (KOH)	7.2 (NMDG)

Concentrations are expressed in mM. The base used for the titration is shown below, in parentheses, for each solution.

pensated. Rm, which was stable 30 s after the whole cell configuration was achieved, was 1.27 ± 0.58 GΩ (n = 26) (Fig 1).

Some recordings were made using the nystatin-perforated patch [11]. Nystatin was prepared in a stock solution containing 60 mg/ml of the antibiotic and, in the case of perforated-patch experiments, it was added to the pipette solution Int. 3 (Table 1) to a final concentration of 150 μg/ml. RBC were voltage-clamped at room temperature with an Axopatch 200B amplifier (Axon Instruments). Stimulation and data acquisition were done using pClamp programs and data were digitised at a sampling interval of 500 μs using a Digidata 1200 Interface (Axon Instruments). The membrane potential was corrected for the potential drop across the access resistance. The analysis of the current activation was done with an exponential fitting procedure utilizing the Clampfit program (Axon Instruments). The currents fitted well to a double exponential equation:

$$I_{(t)} = A_1(1 - \exp^{-t/\tau_1}) + A_2(1 - \exp^{-t/\tau_2})$$

were t = time (ms); A_1 and A_2 = amplitudes (pA); and τ_1 and τ_2 = time constants (ms) of the two exponential components. All the whole-cell currents were corrected off line for the passive ohmic current component that was calculated on each current trace at the intercept of the exponential fitting with the vertical axes positioned at the beginning of the voltage step. The points in Fig. 3B were fitted to the Boltzman equation:

$$G_{\mathrm{Vm}} = 1/(1 + exp^{(V0.5-\mathrm{Vm})/k})$$

where $V_{0.5}$ = midpoint (mV), and k = slope factor (mV). The nonlinear regression was done utilizing Prism 4 (GraphPad Software, Inc.)

2.3. Solutions

The solutions are shown in Table 1. Charybdotoxin (Alomone Lab, Israel) was previously dissolved, at a concentration of 1 μM, in a stock solution (in mM: 100 NaCl, 10 tris[hydroxymethyl]amino-methane (TRIS), 1 ethylenediaminetetraacetic acid (EDTA), 0.1% bovine serum albumine (BSA), pH 7.5). The toxin was used at a final concentration of 20 nM in solution Ext. 1 (Table 1), and perfused extracellularly. Drugs and chemicals were supplied by Sigma (USA).

3. Results

3.1. Human RBC show time- and voltage-dependent outward currents

In about 85% of the patch-clamp whole-cell experiments (n = 86), in addition to a passive current component (not shown in the figures), it was possible to induce a slow-activating, non-inactivating outward current, by means of scaled steps at positive potentials.

Fig. 2A shows the time- and voltage-dependent currents elicited by depolarising the RBC membrane from a holding potential of 0 mV up to 84 mV. No tail currents were observed when the test potential stepped back to 0 mV. The intracellular and extracellular solutions used are reported in Table 1 (Int. 1 and Ext. 1).

The recordings were repeated utilizing the nystatin-perforated patch configuration. In 9 out of 13 cells tested, it was possible to find a similar time- and voltage-dependent outward current at potential steps more positive than 30 mV (Fig. 2B). The current amplitude evoked in these experiments was about 30% to 50% less than the current observed in whole-cell recordings. This can be explained at least in part by the lower K^+ concentration in the pipette solution (Int. 3 in

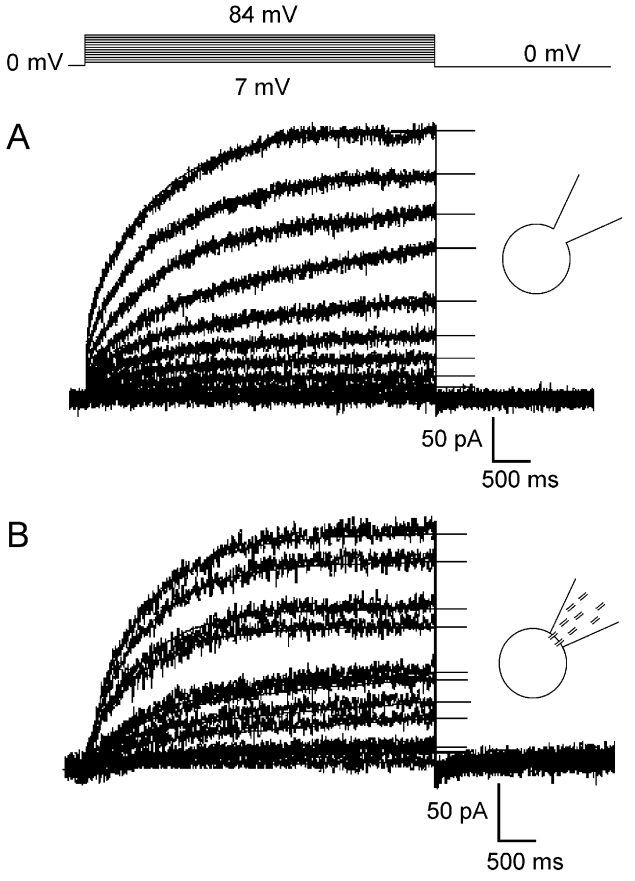

Fig. 2. Voltage-dependent outward currents in human RBC recorded with patch-clamp whole-cell (A) and nystatin-perforated patch (B) techniques. Positive step potentials imposed starting from a holding potential of 0 mV up to 84 mV induced a slow-activating non-inactivating outward current. The current traces have been corrected for the passive current component. Note the different current scales in (A) and (B) (see text). Solutions Int. 1 and Ext. 1 (Table 1) were used in whole-cell experiments (A) and solutions Int. 3 and Ext. 1 (Table 1) were used in nystatin-perforated patch recordings (B). The current activation in (A) and (B) fitted well to the double exponential equation shown in Materials and methods.

Table 1) compared to whole-cell experiments (Int. 1 in Table 1).

3.2. Current-to-voltage relationship, activation parameters and reversal potential

Fitting analysis of the current activation indicates that the rising phase is the sum of two exponential components. The current to voltage relationship ($I–V$) of the total current and of the faster exponential (A_1 in the double exponential equation shown in Materials and methods) were measured from the whole-cell experiments on seven cells and is shown in Fig. 3A. From the same data we calculated the normalised conductance (G) setting the highest value to 1 (Fig. 3B). The half-maximal conductance using a stimulation protocol starting at a holding potential of 0 mV was at about 41.1 mV. The conductance of the faster exponential component was about 46% of total. The time constants of the activation components (τ_1 and τ_2) are plotted as a function of the pulse potentials. τ_1 showed a marked voltage-dependence with a typical bell shape, with maximum value at about 25 mV (Fig. 3C) whereas τ_2, the time constant of the slower component, did not seem to change significantly with voltage (Fig. 3D).

The reversal potential of the voltage-activated currents was obtained by measuring the instantaneous $I–V$ relationship. The stimulus protocol consisted of 5-s conditioning depolarising pulses to 80 mV, to activate the current, followed by membrane repolarisation at scaled potentials between −56 and +56 mV (Fig. 4A). The current intensity measured at the peak immediately after the repolarisation was plotted against the related repolarisation potential (Fig. 4B). Using control solutions Ext. 1 and Int. 1 in Table 1, the equilibrium potential was 3.4 mV (Fig. 4B).

3.3. The voltage-dependent channels were selective for Na^+ and K^+ and regulated by external Cl^-

The ionic selectivity of the channels was studied on 30 RBC. The Nernst potential of the ions in these experiments was: Na^+>100 mV; K^+ = −89 mV; Cl^- = −3 mV; Ca^{2+}>100 mV; Mg^{2+}>100 mV.

Since the only ion with an equilibrium potential compatible with the reversal potential measured was Cl^-, in some experiments we varied its extracellular concentration. The $I–V$ relationship indicated that the reversal potential was unchanged at about 0 mV on lowering the extracellular [Cl^-] from 162 to 50 mM. However, the voltage-dependent current evoked by the depolarising stimulus was reduced by 43% (n = 6; Fig. 4B). A full current recovery was obtained returning to 162 mM Cl^- (not shown).

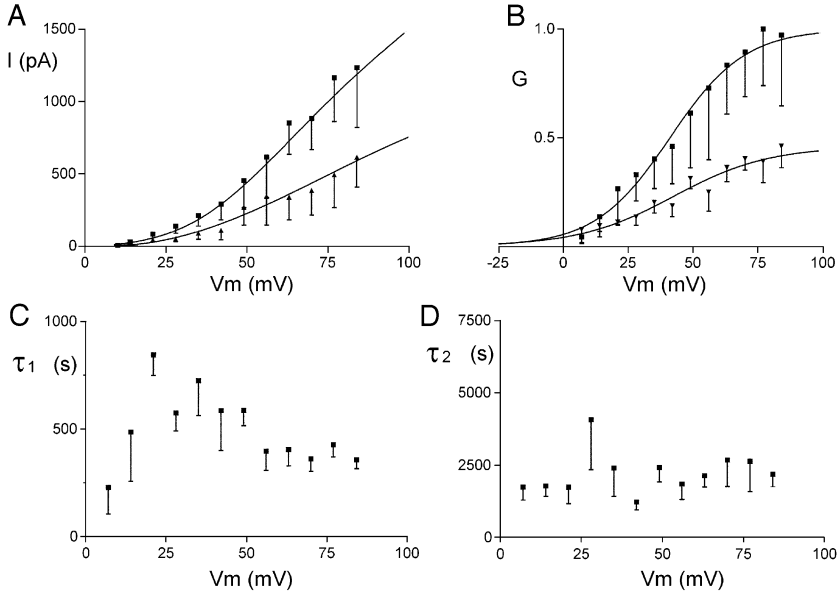

Fig. 3. Biophysical parameters characterising the voltage-dependent outward currents in RBC were derived from patch-clamp whole-cell recordings. (A) The total current (squares) and the faster exponential current component (A_1) from the fitting analysis shown in Fig. 2A (triangles) are plotted as a function of the step potential (Vm). The activation curves in (B) were calculated from the current values: normalised conductance (G) vs. membrane potential (Vm). The points were fitted to the Boltzman equation shown in Materials and methods, where $V_{0.5}$, the midpoint, is 41.1 mV for the total components, and 42.5 for the faster exponential component, and k, the slope factor, is 14.43 and 18.6 mV for the two curves, respectively. The fittings in graph A is the product of the fitting equations in B and the straight line: Gmax (Vm − Erev) where Gmax, the maximum conductance, is 17.4 and 8 nS, respectively, and Erev, the reversal potential, is 3.4 mV (from Fig. 4B). Graphs C and D: the time constants τ_1 and τ_2 of the two exponential current components (see text) are plotted against the membrane potential (Vm). Note the typical bell shape of τ_1 whereas τ_2 does not seem to change significantly with voltage. Each data point in the graphs represents the mean ± S.E. of seven cells.

With regard to the monovalent cations, a change in Na^+ or K^+ gradients across the membrane did modify the reversal potential measured by $I–V$ curves in eight cells. The voltage-stimulus protocol consisted of a depolarising ramp rising from -50 mV at the rate of 10 mV·s^{-1}. We used a low [K^+] internal solution (Int. 4; Table 1) vs. three different extracellular solutions. When the external Na^+ or K^+ concentrations were higher than the internal ones (Ext. 1 or Ext. 5; Table 1), the reversal potential shifted to positive values, whereas when both [Na^+] and [K^+] were balanced across the membrane (Ext. 4; Table 1) the reversal potential was zero (Fig. 5).

These findings imply that the channels are permeable to Na^+ and K^+ and not to Cl^- ions.

To rule out a possible implication of the Ca^{2+}-activated K^+ channels, the Gardos, the voltage-dependent outward current was also evoked in Ca^{2+}-free solutions (Int. 2, Ext. 2 in Table 1; $n=6$), in presence of charybdotoxin in the external solution (20 nM; $n=8$) or TEA

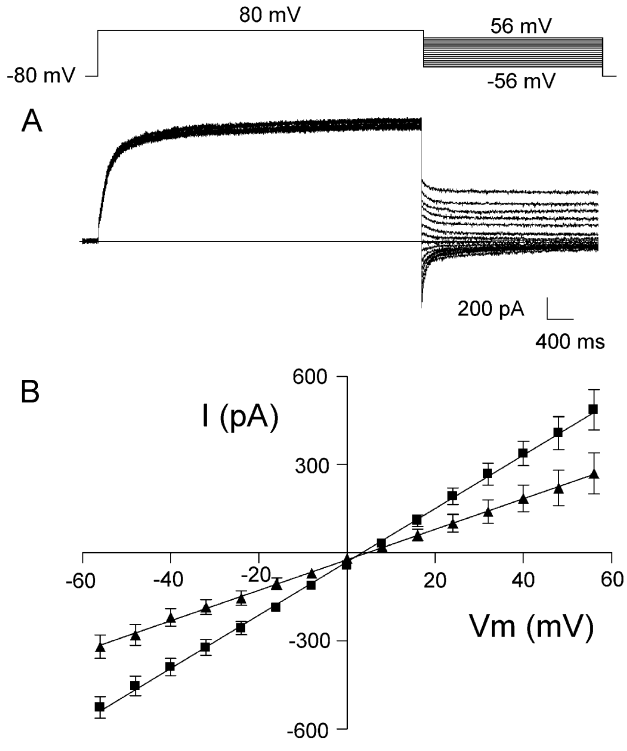

Fig. 4. The reversal potential of the outward current was evaluated by an instantaneous $I–V$ plot. (A) The stimulus protocol consisted of a depolarising step potential at 80 mV, to activate the voltage-dependent currents, followed by a repolarisation to scaled potentials. The tail currents were measured at the peak after subtraction of the passive current component. (B) The mean values from 10 cells ± S.E. were plotted against the potential of repolarisation (squares) and fitted with a straight line. The reversal potential was 3.4 mV (solution Ext. 1 and Int. 1 in Table 1). In six of these cells the extracellular Cl^- concentration was varied from 162 to 50 mM (triangles; solution Ext. 3 in Table 1). The reversal potential did not change to positive values as expected if Cl^- carries the voltage-dependent currents.

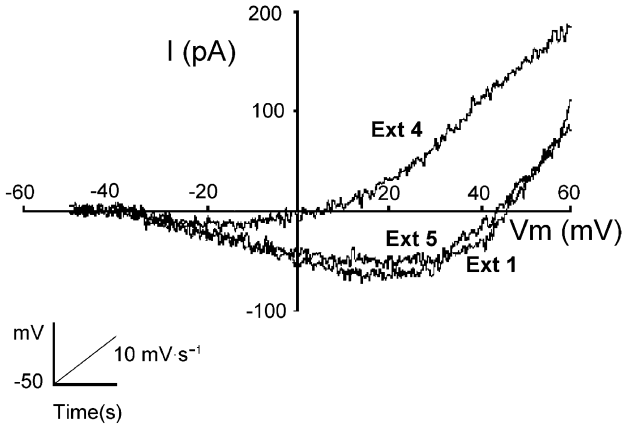

Fig. 5. The voltage-dependent channels are selective for Na^+ and K^+. To study the permeability of these channels to Na^+ and K^+, the Na^+ and K^+ gradients across the membrane were varied and the changes in reversal potential were measured by $I–V$ curves. The voltage-stimulus protocol (insert) consisted of a depolarising rising ramp from -50 mV at the rate of 10 mV·s^{-1}. A low [K^+] internal solution (Int. 4; Table 1) was used. When the external Na^+ (solution Ext. 1; Table 1) or K^+ (solution Ext. 5; Table 1) was higher than the internal one, the reversal potential shifted to positive values, whereas when both [Na^+] and [K^+] were balanced across the membrane (Ext. 4; Table 1) the reversal potential was zero.

(20 mM, solution Ext. 6 in Table 1; $n=7$). No inhibitory effects were observed (data not shown). Ruthenium red (10 μM) added to the external medium did not inhibit this current.

4. Discussion

Membrane currents in human RBC have been studied by means of whole-cell and nystatin-perforated configurations of the patch-clamp technique. These cells, in addition to a passive current component, not taken into account in these studies, have a quite large slowly activating non-inactivating time- and voltage-dependent outward current carried by Na^+ and K^+ ions (I_{NSC}). This current is reduced following a partial substitution of extracellular Cl^- by tartrate.

We can exclude that the outward current, normally activated at very positive potentials, was due to membrane damage, since it was voltage- and time-dependent, and selectively carried by Na^+ and K^+. This indicates that it was not the result of nonspecific membrane breakdown. Furthermore, the current was also evoked during perforated-patch recordings. This technique minimizes the washout of cytosolic constituents. Under these experimental conditions, the reversal potential at 0 mV and the voltage-dependent characteristics were identical to the observation in the whole-cell configuration.

That voltage-dependent K^+ channels are involved has been excluded since TEA did not affect the currents described in this paper [12,13]. Ca^{2+}-dependent K^+ channels have been described in RBC [14]. Charybdotoxin, a scor-

pion toxin that blocks these channels in RBC [15], together with Ca^{2+}-free experiments, was used to exclude their involvement in the generation of the voltage-dependent outward currents that persisted also under these conditions. Furthermore, the Ca^{2+}-dependent K^+ channels present in human RBC are not voltage-dependent and the reversal potential observed here excludes the involvement of selective K^+ channels.

Ruthenium red, reported to partially inhibit a Na^+ and K^+ conductance increase induced by long-lasting changes in membrane potential to positive voltages in human RBC [4], does not affect the current described in this paper. This observation may suggest that other cationic currents are evoked as a consequence of a long-lasting positive voltage imposed to the RBC membrane.

The activation of the whole-cell currents fitted well to double exponential curves. This behaviour may reflect the different open states of the channels observed in single channel recordings [5]. Only the time constant of the faster exponential component showed a clear voltage-dependence and a bell-shaped $\tau-V$ curve as predicted by the Hodgkin and Huxley model. However, we cannot completely rule out a certain voltage-dependence of the slower component since, under our experimental conditions, this current component might have the bell-shaped portion of the $\tau-V$ curve around the reversal potential (i.e. where the driving force and thus the currents through the open channels are negligible and the time constant cannot be reliably estimated).

The whole-cell current shown here shares certain characteristics with the single-channel currents previously described in RBC [6]. They show slow activation and deactivation kinetics, no inactivation, and identical Na^+ and K^+ permeability. The activation curve suggests that this voltage-dependent current begins to be active at a slightly negative potential, close to the resting potential, estimated between -5 and -15 mV [16]. The sigmoidal curve increases less steeply and the midpoint is at a less positive potential than that calculated from single channel data [7]. These small discrepancies may be due to the differences in experimental conditions. Assuming 300 channels per RBC, an opening probability of about 80%, and a single channel conductance of 35 pS [7,19], the theoretical whole-cell maximum conductance should be 8.4 nS, very close to the fitting value found in Fig. 3A for the faster exponential current component.

An interesting feature of the channel is the increasing open probability passing from physiological concentrations up to 500 mM salt [5,6]. This was attributed to different KCl concentrations [7]. These observations can be better explained on the bases of our finding that the voltage-dependent outward current decreases on lowering the external Cl^- from 162 to 50 mM, maintaining unchanged the K^+ concentration (Fig. 4). Since the current decrease occurs with no change in the reversal potential, it may be attributed to a modulatory effect of Cl^- ions on the voltage-dependent cation channels.

Interestingly enough, both extracellular and intracellular Cl^- dependence of NSC shrinkage-activated currents has been observed in various cell types. NSC currents are reported to be reduced as the extracellular Cl^- is partially replaced by aspartate in airway epithelia [17]. In human RBC, replacement of external Cl^- by gluconate as well as an increase in pipette Cl^- decreased the outward shrinkage-activated NSC currents [18].

4.1. Physiological considerations

NSC channels belong to a channel family that has been proposed to play a role in various regulatory functions. Osmotic cell shrinkage activates NSC channels in a variety of cell types [20] suggesting the participation of these channels in cell volume regulation. Recent data show that NSC channels in human RBC can be activated by prostaglandin E_2 suggesting a function in blood clot formation. [21]

RBC are subjected to widely differing conditions in the circulation. For instance, they pass in a few seconds from 300 up to 1400 mosM during their transit through the vasa recta in the kidney. They must also adapt to rapid changes in volume and shape when they flow from arterioles to capillaries. These changes require great adaptability. Changes in ionic gradients across their membrane and stretch activation of cation channels [22,23] might alter the membrane potential sensed by the voltage-dependent cation channels. In turn, these channels can open with a time constant consistent with the rapid changes required by the circulation.

We cannot say why a 15% of RBC does not show the NSC conductance in the present study. This lack of the NSC current in this RBC fraction does not seem to be due to the ageing process of RBC population (unpublished data). If these currents are involved in clot formation [21], then we should conclude that not all RBC share the same functions in coagulation.

Acknowledgements

We wish to thank Drs. A. Brovelli and A. Arduini for helpful discussions, and I. Cino for testing TEA on these currents. The research was supported by Sigma Tau S.p.a. (Italy).

References

[1] P. La Celle, A. Rothstein, The passive permeability of the red blood cell to cations, J. Gen. Physiol. 50 (1966) 171–188.
[2] G.S. Jones, P.A. Knauf, Mechanism of the increase in cation permeability of human erythrocytes in low-chloride media, J. Gen. Physiol. 86 (1985) 721–738.
[3] J.A. Donlon, A. Rothstein, The cation permeability of erythrocytes in low ionic strength media of various tonicities, J. Membr. Biol. 1 (1969) 37–52.

[4] J.A. Halperin, C. Brugnara, M.T. Tosteson, T. Van Ha, D.C. Tosteson, Voltage-activated cation transport in human erythrocytes, Am. J. Physiol. 257 (1989) C986–C996.
[5] P. Christophersen, P. Bennekou, Evidence for a voltage-gated, non-selective cation channel in the human red cell membrane, Biochim. Biophys. Acta 1065 (1991) 103–106.
[6] L. Kaestner, C. Bollensdorff, I. Bernhardt, Non-selective voltage-activated cation channel in the human red blood cell membrane, Biochim. Biophys. Acta 1417 (1999) 9–15.
[7] L. Kaestner, P. Christophersen, I. Bernhardt, P. Bennekou, The non-selective voltage-activated cation channel in the human red blood cell membrane: reconciliation between two conflicting reports and further characterisation, J. Bioelectr. 52 (2000) 117–125.
[8] S.J. Korn, A. Marty, J.A. Connor, R. Horn, Perforated patch recording, Methods Neurosci. 4 (1991) 264–373.
[9] O.P. Hamill, A. Marty, E. Neher, B. Sakman, F. Sigworth, Improved patch-clamp techniques for high resolution current recording from cells and cell-free membrane patches, Pfluegers Arch. 391 (1981) 85–100.
[10] D.A. Berk, R.M. Hochmuth, R.E. Waugh, Viscoelastic properties and rheology, in: P. Agre, J.C. Parker (Eds.), Red Blood Cell Membrane: Structure, Function, Clinical Implications, Marcel Dekker, New York, 1989, pp. 423–454.
[11] J.Y. Cheung, X.Q. Zhang, K. Bokvist, D.L. Tillotson, B. Miller, Modulation of calcium channels in human erythroblasts by erythropoietin, Blood 89 (1997) 92–100.
[12] N.A. Castle, D.G. Haylett, D.H. Jenkinson, Toxins in the caracterization of potassium channels, TINS 12 (1989) 59–65.
[13] G.J. Kaczorowski, M.L. Garcia, Pharmacology of voltage-gated and calcium-activated potassium channels, Curr. Opin. Chem. Biol. 3 (1999) 448–458.
[14] R. Grygorczyk, W. Schwarz, H. Passow, Ca^{2+}-activated K^+ channels in human red cells. Comparison of single-channel currents with ion fluxes, Biophys. J. 45 (1984) 693–698.
[15] D. Wolff, X. Cecchi, A. Spalvins, M. Canessa, Charybdotoxin blocks with high affinity the Ca-activated K+ channel of Hb A and Hb S red cells: individual differences in the number of channels, J. Membr. Biol. 106 (1988) 243–252.
[16] J.F. Hoffman, P.C. Laris, Determination of membrane potentials in human and Amphiuma red blood cells by means of fluorescent probe, J. Physiol. 239 (1974) 519–552.
[17] H.C. Chan, D.J. Nelson, Chloride-dependent cation conductance activated during cellular shrinkage, Science 257 (5070) (1992) 669–671.
[18] M.H. Huber, N. Gamper, F. Lang, Chloride conductance and volume-regulatory nonselective cation conductance in human red blood cell ghosts, Pflugers Arch.-Eur. J. Phys. 441 (2001) 551–558.
[19] P. Bennekou, The voltage-gated non-selective cation channel from human red cells is sensitive to acetylcholine, Biochim. Biophys. Acta 1147 (1993) 165–167.
[20] J.-P. Koch, C. Korbmacher, Mechanism of shrinkage activation of nonselective cation channels in M-1 mouse cortical collecting duct cells, J. Membr. Biol. 177 (2000) 231–242.
[21] L. Kaestner, I. Bernhardt, Ion channels in the human red blood cell membrane: their further investigation and physiological relevance, J. Bioelectr. 55 (2002) 71–74.
[22] R.M. Johnson, K. Tang, Induction of a Ca(2+)-activated K+ channel in human erythrocytes by mechanical stress, Biochim. Biophys. Acta 1107 (1992) 314–318.
[23] R.M. Johnson, Membrane stress increases cation permeability in red cells, Biophys. J. 67 (1994) 1876–1881.